RESEARCH ARTICLE `OPEN ACCESS`

Rapid At-Line AAVX Affinity HPLC: Enabling Process Analytical Technology for Bioprocess Development of Adeno-Associated Virus Vectors

Jakob Heckel[1] 🆔 | Timo Bohlig[2] | Lea Bonnington[1] | Michael Leiss[1] | Markus Haindl[2] | Jürgen Hubbuch[3] | Tobias Graf[1]

[1]Pharma Technical Development Analytics, Roche Diagnostics GmbH, Penzberg, Germany | [2]Gene Therapy Technical Development, Roche Diagnostics GmbH, Penzberg, Germany | [3]Institute of Process Engineering in Life Sciences, Section IV: Biomolecular Separation Engineering, Karlsruhe Institute of Technology, Karlsruhe, Germany

Correspondence: Jakob Heckel (jakob.heckel@roche.com)

ABSTRACT

Recombinant adeno-associated virus (rAAV) vectors have emerged as a new class of therapeutic modal with the promise to treat or even cure hereditary and acquired diseases, but their consistent and efficient production remains challenging. To address these inadequacies, the implementation of process analytical technology (PAT) principles for the development of rAAV-based gene therapies holds the prospect of promoting greater product and process understanding. However, a substantial lack of suitable analytical tools during both upstream and downstream processing (DSP) hinders the ability to fully realize the potential of PAT for rAAVs. To fill this gap, our recently described AAVX affinity-based high-performance liquid chromatography (HPLC) method was assessed as an at-line PAT tool to determine the capsid titer and the percentage of filled capsids at various stages of the production process. Leveraging the fast and robust provision of these parameters, even for challenging samples, the benefits of this approach for improved process monitoring and control were demonstrated for samples generated both during fermentation and DSP. Given the versatility of our developed analytical method for different rAAV serotype and payload combinations, we eventually highlight its expansive opportunities to streamline process development and therefore contributing to high-quality and cost-efficient production of rAAV-based gene therapies.

1 | Introduction

The development of in vivo gene therapies using viral vectors shows auspicious treatment options for various genetic diseases with high unmet medical need. Among the most prominent gene delivery vectors are recombinant adeno-associated virus (rAAV) vectors. Their potential is reflected in the rising numbers of these molecular entities already approved or being evaluated in (pre-)clinical studies due to the permanence of gene expression,

a broad range of tissue tropisms and low immunogenicity [1, 2]. Despite intense research and development efforts, process and mechanistic understanding of rAAV manufacturing is limited compared to well-established biopharmaceuticals such as monoclonal antibodies [3, 4]. In this context, hurdles with regard to low yield and purity during bioprocessing as well as varying potency of the final product are yet to be resolved to ensure reproducible, safe, and efficient production of rAAV-based gene therapies [3]. An important step towards understanding and

controlling these aspects involves improved knowledge of the manufacturing process itself. Generally, a process is considered well-understood when all allegedly critical sources of variability are identified and can be controlled to meet consistently the quality target product profile. Furthermore, in a well-understood process, quality attributes should be predictable based on process knowledge with sufficient accuracy and reliability over the design space conditions for risk-based process control [5].

To this end, process analytical technology (PAT), as outlined by the FDA initiative first published in 2004, and further adapted within the ICH guideline Q8 (R2), can be understood as a systematic approach to establish and monitor critical process parameters (CPPs) and critical quality attributes (CQAs) for (bio-)pharmaceutical manufacturing. Ultimately, the goal of PAT is to enable real-time process monitoring and control, thereby achieving consistent product quality and hence ensuring patient safety. Additionally, the benefits of implementing PAT tools are an enhanced product and process understanding by exploiting the vast number of generated data, and the prospect of improved productivity and minimized risk of batch failures. Eventually, these optimizations can contribute to a positive environmental impact and cost efficiency [5].

In the field of rAAV-based gene therapies, CPPs and their impact on CQAs are only poorly understood due to the lack of prior knowledge or developments [4]. Important product-related quality attributes of rAAV products are capsid titer and genomic titer, also represented as the ratio of full to total capsids (%full) [6, 7]. Reported analytical methods for rAAVs claiming potential for PAT applications largely focus either on upstream processing (USP) or do not state the intended use case at all [8–10]. Most of the proposed USP methods for viral vectors are based on soft sensors that exhibit considerable drawbacks in terms of repeatability [11, 12]. By contrast, no suitable approach specifically intended for rAAV downstream processing (DSP) has been described to date. This may be due to the applied analytical methods runtimes that do not allow a sufficient turnaround time (TAT) for DSP monitoring. Various rapid methods in PAT applications for conventional large molecules are spectroscopy-based, like RAMAN, fluorescence, or UV absorption [8]. These methods alone often do not provide the necessary specificity to distinguish the rAAV signal from impurity signals. This issue can be adressed by physically separating different species, as, for example, achieved by chromatography-based methods such as high-performance liquid chromatography (HPLC). Although being considered as too slow until recently, advances in columns and instrumentations have promoted the implementation of fast HPLC methods with reasonable TATs, while maintaining a high level of accuracy and precision [13].

Exploiting these beneficial features, this study evaluates the potential of a fast affinity-based HPLC method as a PAT tool to determine capsid titer and %full of various rAAV serotypes based on the obtained A_{260}/A_{280} ratio and the fluorescence signal using product-specific calibration curves. As demonstrated for multiple processing steps for both USP and DSP applications, this approach provides process engineers additional insights into individual unit operations with a clear time advantage compared to analytical offline workflows.

2 | Materials and Methods

2.1 | Eluents

All eluents were prepared using ultrapure water and analytical-grade chemicals. Tris(hydroxymethyl)-aminoethane hydrochloride (Tris-HCl), sodium chloride (NaCl), magnesium chloride hexahydrate ($MgCl_2 \times 6H_2O$), sorbitol, and hydrochloric acid (HCl) were obtained from Merck (Darmstadt, Germany). Glycine hydrochloride and 10% Pluronic F-68 were purchased from Thermo Fisher Scientific (Waltham, MA, USA).

Eluent A: 25 mM Tris-HCl, 100 mM NaCl, 2 mM $MgCl_2$, 0.1% Sorbitol 0.005% Pluronic, pH 7.8

Eluent B: 100 mM Glycine-HCl, 250 mM $MgCl_2$, pH 2.35

2.2 | Hardware and Method Parameters

Affinity HPLC was performed using an Agilent Technologies LC system (Santa Clara, CA, USA) as described in our previous publication [13]. To increase limit of detection, a UV diode array detector (DAD) (G7117B) equipped with a 60 mm Max-Light Cartridge Cell (4 µL; G4212-60007) was installed. Short analytical columns (NovoGROM, 2 mm × 20 mm) packed with POROS CaptureSelect AAVX affinity resin (Thermo Fisher) were purchased from Dr. Maisch (Ammerbuch, Germany).

The initially developed method had a run-time of 4 min. Optimization of the previously reported eluents allowed a more efficient binding onto the column during the load phase and a sharper elution peak of the entire rAAV fraction (total capsids). This was achieved by slightly adjusting the pH of both mobile phases A and B. Additionally, a flow ramp during the first 0.5 min after injection increased residence time of the sample on the column thus enhancing binding conditions. Furthermore, we were able to significantly reduce the volume needed for the wash step after injection as well as column equilibration after elution. Consequently, by employing higher flow rates the method was shortened to a run time of 2 min (Table 1). Method performance was tested and confirmed with various serotypes (e.g., rAAV2, rAAV8, and rAAV9). Applied injection volumes varied in between 2 and 100 µL, based on their expected concentration, and spanned a theoretical column load of 2E10 to 7E12 capsids/mL resin. An exemplary representation of various chromatograms from process samples is shown in S1.

2.3 | Reference Analytical Methods

2.3.1 | Size Exclusion Chromatography Coupled to Multi-Angle Light Scattering (SEC-MALS) Detection

SEC-MALS was used as a reference method for capsid titer and %full. Analysis of samples was performed using the same instrumental setup and method as described previously [13].

TABLE 1 | Timetable of the utilized AAVX affinity HPLC method (1 CV = 40 μL).

Step	Eluent A (%)	Eluent B (%)	Time (min)	Flow (mL/min)	Column volumes (CV)	Linear velocity (cm/s)
Injection	100	0	0	0.1		0.08
Binding	100	0	0–0.5	0.1–2	12	0.08–1.67
Wash	100	0	0.5–1	2	24	1.67
Elution	0	100	1–1.6	1.87	27	1.56
Equilibration	100	0	1.6–1.85	2	12	1.67
	100	0	1.85–2	2–0.1	3.8	1.67–0.08

2.3.2 | Mass Photometry (MP)

MP was utilized for characterization of rAAVs to differentiate empty, partially filled, and full capsids [14, 15]. For preparation, samples were diluted in PBS, applied onto cleaned microscope coverslips, and placed on the SamuxMP (Refeyn Ltd., Oxford, UK). Movies were recorded using the AcquireMP software. The resulting histograms were analyzed by applying Gaussian curve fitting to derive the capsid composition of each sample. For a more detailed method description, we refer to Ebberink et al. [14].

2.4 | Production of Recombinant Adeno-Associated Virus Vectors

Two distinct in-house serotypes (rAAV α and rAAV β) were used for this study. Each serotype carried a payload varying in its size and encoded transgene (Payload 1 and Payload 2). HEK293 cells were cultivated in fed-batch mode until the desired viable cell density (VCD) was achieved. Subsequently, triple transfection was conducted by adding a premixed combination of transfection reagents and plasmid media. rAAVs were harvested applying a lysis protocol, involving the addition of Triton X-100 (0.5%) and Benzonase (50 U/mL) followed by incubation for 60 min at 37°C [16]. After rAAV release, the harvest was clarified through depth filtration and subsequently purified.

2.5 | Sample Preparation of USP Material

During fermentation of rAAV β, regular samples of the cell culture fluid (CCF) were obtained for further analysis. The first sample was drawn 24 h after transfection, and subsequent samples were collected on a daily basis. The final sample was taken after 96 h of fermentation prior to harvest. To avoid unintended cell lysis by freezing and thawing, 1 mL aliquots of each sample were directly processed by either filtrating utilizing Sartorius Minisart 0.22 μm 6.2 cm^2 syringe filters (Göttingen, Germany) or centrifugation for 10 min at 140,00 rpm (RCF = 18,800 × g) using a Micro Star 21 centrifuge (VWR, Radnor, PA, USA). Filtrate and supernatant as well as additional aliquots of unprocessed samples were stored at −80°C until harvest. For analysis all collected samples were thawed. The previously unprocessed samples were then lysed using the protocol above and subsequently either filtered or centrifuged as described (Figure 1A). In total, 16 samples were obtained and analyzed in duplicate to determine the rAAV titer before and after lysis, as well as to compare the effects of sample pretreatment via centrifugation or filtration.

2.6 | Assessed DSP Unit Operations

DSP of the two serotypes, the load material as well as the target pool(s) were sampled for AAVX Affinity HPLC analysis as shown in Figure 1B. Additional samples were stored for later offline reference lab analytics. Additionally, the capability of the method to measure more complex samples originating from flow-through (FT), wash, and high-salt cleaning in place (CIP) steps was also tested during polishing.

2.6.1 | Concentration via Filtration

After cell lysis, the harvested cell culture fluid (HCCF) was stored at 4°C for 24 h. It was then concentrated and diafiltrated using a Tris-based buffer with a pH value of 7.4 by utilizing a Sartoflow Beta (Sartorius) modular filtration system equipped with a 100 kDa cutoff filter cassette. The resulting concentrated cell culture harvest was further filtered employing Sartoclean CA Maxicaps (Sartorius) 0.8–0.2 μm filters.

2.6.2 | Affinity Purification of rAAVs

Affinity purification was performed to remove process-related impurities, such as host cell proteins and DNA. Therefore, the concentrate was loaded onto a POROS CaptureSelect AAVX Affinity column (Thermo Fisher) installed on an ÄKTA Pilot (Cytiva, Marlborough, MA, USA). Elution from the column was achieved using a glycine-based buffer at pH 2.5. The column was subsequently stripped and cleaned using phosphoric acid and guanidine buffers and stored in 20% ethanol [17]. The affinity pool obtained from the elution step was instantly neutralized to pH 8 using 2 M Tris buffer.

2.6.3 | Polishing Step via Anion-Exchange Chromatography (AEX)

To enrich DNA containing capsids, a two-step AEX chromatography step was performed employing an ÄKTA Avant (Cytiva) system. Elution was carried out using a pH 8 Tris buffer. By
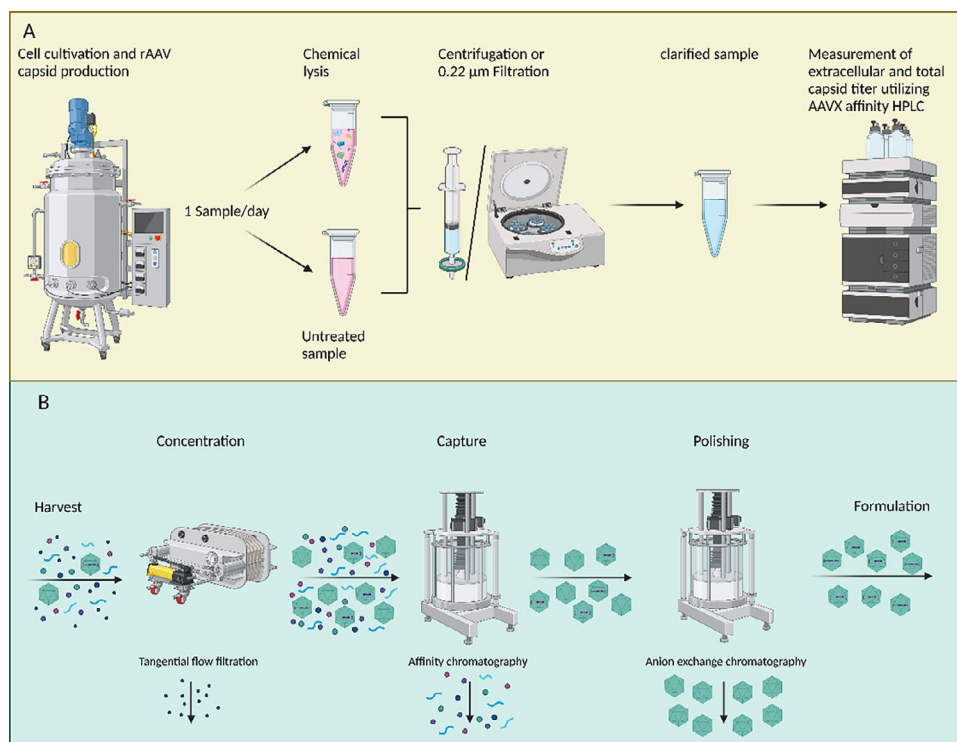
FIGURE 1 | Overview of process samples analyzed with AAVX affinity HPLC. (A) For USP, samples were drawn each day and processed with/without cell lysis as well as subsequent clarification via centrifugation or filtration. (B) DSP samples were drawn at-line from the process before and after TFF, affinity chromatography, and anion-exchange chromatography. DSP, downstream processing; HPLC, high-performance liquid chromatography; TFF, tangential flow filtration; USP, upstream processing.

increasing the amount of salt in the elution buffer, empty and filled capsids were eluted separately. The column was then stripped using a high salt buffer and subsequently cleaned and stored in 0.1 M NaOH.

3 | Results and Discussion

3.1 | Calibration for Different Serotype/Payload Combinations

Our previously published AAVX affinity HPLC method takes advantage of the high selectivity of the POROS CaptureSelect AAVX affinity resin towards several different AAV serotypes [13, 17]. Packed in short analytical columns, it allows the efficient isolation of the entire rAAV fraction from complex samples, irrespective of the presence or absence of a payload. For analysis, the intrinsic fluorescence of tryptophan residues in the elution peak is acquired to calculate the capsid titer. Additionally, UV detection of protein and DNA absorbance (A_{260} and A_{280}) allows for determining the DNA content of the eluting capsids. For this, it is assumed that the fluorescence properties are serotype-specific as they depend on the protein conformation and amino acid sequence as well as on the local environment of the tryptophan residues [18, 19]. By contrast, UV absorbance is influenced by the specific characteristic of the capsid as well as the DNA payload and is therefore not only linked to the amino acid sequence of the rAAV but, additionally, to the DNA payload size. Accordingly, the combination of UV and FLR detection allows

for the determination of capsid titer and %full after establishing a calibration for each serotype/payload combination.

Our proposed calibration procedure is generally performed with two stock solutions ("Empty" and "Full") for each investigated rAAV construct, with capsid titer and %full derived from reference analytics. We chose to utilize SEC-MALS as reference method in this study due to its capability to determine the capsid titer as well as %full simultaneously in a single measurement with good accuracy and low sample material requirements [20, 21]. To account for the DNA-dependent quenching effect, the calibration of the fluorescence response is conducted applying a dilution series of a virus stock sample containing only empty capsids, henceforth referred to as "Empty"-stock. For UV based %full calibration, the "Full"-stock (containing a well-defined, high amount of filled capsids) is mixed with the "Empty"-stock in distinct steps to obtain different full/empty ratios. For a more detailed description of the different calibration steps see also [13].

Considering the plethora of possible serotype/payload combinations, creating a complete calibration set for each rAAV of interest would be utterly laborious and resource-intensive. To address this challenge we aimed to develop a generic protocol that enables recalibration of existing calibration data utilizing only two samples of a new serotype/payload combination, one sample containing mainly empty capsids, while the other one preferably features a high content of filled capsids. This approach involves determining three correction factors (CF) which are elaborated upon below to provide a comprehensive understanding.
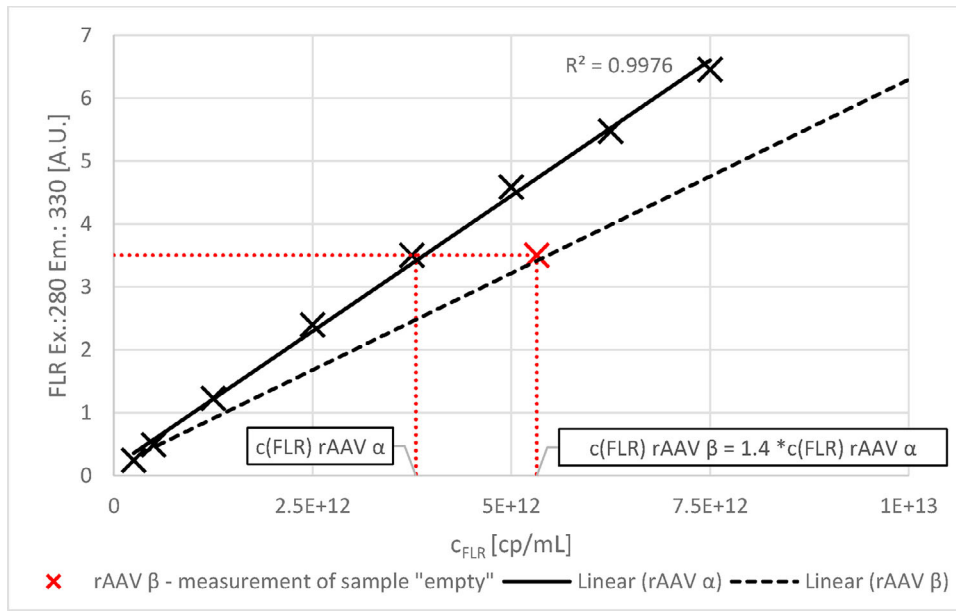
FIGURE 2 | Correction of the fluorescence intensity based on an existing calibration. The linear regression of rAAV α (solid black line) is utilized to derive the calibration of noncalibrated rAAV β (dotted black line) by applying a correction factor CF_{Fluor} of 1.4. This CF_{Fluor} was calculated by comparing the SEC-MALS referenced capsid titer of an empty sample from rAAV β (red cross) to the existing calibration of rAAV α. CF_{Fluor}, fluorescence correction factor; rAAV, recombinant adeno-associated virus; SEC-MALS, size exclusion chromatography coupled to multi-angle light scattering.

3.1.1 | Fluorescence Correction Factor (CF_{Fluor})

Compared to other proteins, all rAAV serotypes contain an abundance of tryptophan residues, affording their analysis with high sensitivity based on the intrinsic fluorescence signal. Yet, total protein concentrations of rAAV in-process samples typically fall below 0.1 mg/mL [22]. The inner filter effect, compromising the linearity of the signal response, is consequently negligible for rAAVs. Accordingly, the measured fluorescence intensity is dependent on the amount of tryptophan residues, which in turn correlates with the concentration of rAAV capsids in the sample.

To allow for the adaptation of an existing calibration, the fluorescence response of a sample containing mainly empty capsids of the noncalibrated serotype is compared to the previously known serotype via a single-point calibration. The hereby obtained CF_{Fluor}, is then applied to the existing calibration (e.g., rAAV α) to calculate the titer of another serotype (e.g., rAAV β). For example, it was observed that rAAV β showed approximately 30% less fluorescence per capsid than rAAV α resulting in a CF_{Fluor} of 1.4 (Figure 2).

3.1.2 | Quenching Correction Factor (CF_{Quench})

Although the exact mechanism behind the observed DNA payload-dependent capsid fluorescence quenching effect is not yet fully understood, it appears to be specific for the capsid/payload combination. For several serotypes tested, our findings indicate a linear relationship between the corresponding quenching to the fraction of filled capsids in a sample (data not shown). To take this effect into account, a Stern-Volmer approach can be employed to correct the measured fluorescence intensity based on the %full value and a serotype/payload-specific correction factor (CF_{Quench})

$$c_{rAAV} = c_{FLR} * \left(\frac{\%full * CF_{Quench}}{100} + 1 \right) \tag{1}$$

where c_{FLR} describes the calculated uncorrected titer derived from the fluorescence signal of a given sample based on empty capsid calibration.

To determine the serotype-payload-specific CF_{Quench} for the investigated serotype, we conducted an experimental comparison between the titer obtained by SEC-MALS and the uncorrected fluorescence response of full samples for both rAAV α and rAAV β. For rAAV α, the derived CF_{Quench} of 3.6 suggested a total quenching of approximately 80% of the fluorescence in a filled capsid of the rAAV α/Payload 1 combination. By contrast, the rAAV β/Payload 2 combination showed less quenching (approximately 30%) resulting in a factor of 0.6.

3.1.3 | UV-ratio Correction Factor ($CF_{UV-ratio}$)

The calculation of the amount of capsids filled with the DNA payload is based on the A_{260}/A_{280} UV ratio [23]. In this approach, the absorbance of DNA at 260 nm is put in relation to the absorbance of protein at 280 nm. As the UV signals for the payload DNA and capsid protein overlap at both wavelengths, the A_{260}/A_{280} ratio is calculated as described in Equation (2)

$$\frac{A_{260}}{A_{280}} = \frac{A_{260, \text{DNA}} + A_{260, \text{Capsid}}}{A_{280, \text{DNA}} + A_{280, \text{Capsid}}} \tag{2}$$

Plotting the %full derived from reference analytics against the determined A_{260}/A_{280} ratio eliminates the codependence of both
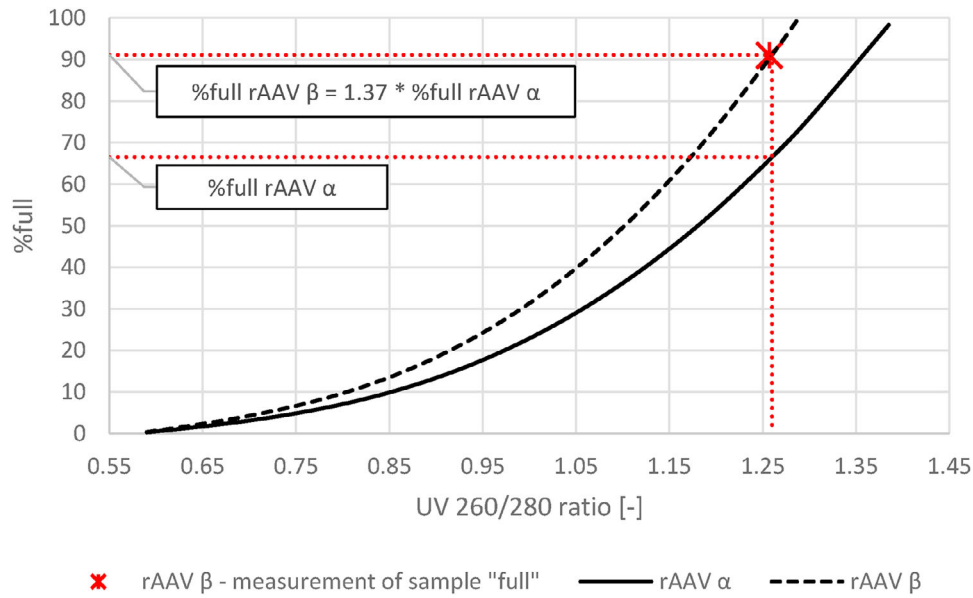
FIGURE 3 | Correction of quenching effect for different rAAVs. The %full calibration curve of rAAV α (solid black line) was adjusted for rAAV β (dotted black line) by applying a correction factor CF$_{\text{UV-ratio}}$ of 1.37. This CF$_{\text{UV-ratio}}$ was calculated as shown in Equation (7) by analyzing a single, SEC-MALS referenced sample of rAAV β containing filled capsids (indicated as red cross). CF$_{\text{UV-ratio}}$, UV-ratio correction factor; rAAV, recombinant adeno-associated virus; SEC-MALS, size exclusion chromatography coupled to multi-angle light scattering.

UV signals and leads to a serotype- and payload-specific %full calibration curve (Figure 3).

A linear relationship between the absorbance of an analyte at a specific wavelength λ and its concentration c is given by the Beer–Lambert law

$$A_\lambda = \varepsilon_\lambda * l * c \qquad (3)$$

with l being the path length and ε_λ the wavelength-specific molar absorption coefficient of the analyte.

The concentration of payload DNA can be calculated utilizing the total capsid titer (c_{rAAV}) and the percentage of filled capsids (%full) (Equation 4).

$$c_{\text{Payload}} = c_{\text{rAAV}} * \%\text{full} \qquad (4)$$

when combining Equations (2)–(4), it is noticeable that the A_{260}/A_{280} ratio is independent of the capsid concentration, but the corresponding %full has to be specifically determined for different serotype and payload combinations (Equation 5) due to the specific absorption coefficients.

$$\frac{A_{260}}{A_{280}} = \frac{\varepsilon_{260,\,\text{Payload}} * \%\text{full} + \varepsilon_{260,\,\text{Capsid}}}{\varepsilon_{280,\,\text{Payload}} * \%\text{full} + \varepsilon_{280,\,\text{Capsid}}} \qquad (5)$$

Although the A_{260}/A_{280} ratio relies on the composition of amino acids and nucleic acids of the analyte, a ratio of 0.6 is generally accepted for pure protein and $\approx$1.8 for pure DNA, at least it is considered to be constant for different rAAV capsids and payloads. Considering the two components (i.e., DNA payload and capsid protein) separately allows for a representation of the absorption coefficients for each as a function of only one

wavelength.

$$\varepsilon_{260,\,\text{Payload}} = \varepsilon_{280,\,\text{Payload}} * 1.8$$

$$\varepsilon_{280,\,\text{Capsid}} = \varepsilon_{260,\,\text{Capsid}}/0.6 \qquad (6)$$

assuming that the same A_{260}/A_{280} ratio value is measured for two different rAAV variants, the %full of one of the two serotypes (ST2) can be calculated in relation to the existing calibration data of the other serotype (ST1) combining Equations (5) and (6)

$$\%\text{full}_{\text{ST2}} = \%\text{full}_{\text{ST1}} * \frac{\varepsilon_{280,\,\text{Capsid, ST2}}}{\varepsilon_{280,\,\text{Capsid, ST1}}} * \frac{\varepsilon_{260,\text{Payload, ST1}}}{\varepsilon_{260,\text{Payload, ST2}}}$$

$$= \%\text{full}_{\text{ST1}} * \text{CF}_{\%\text{full}} \qquad (7)$$

This enables adjusting the existing A_{260}/A_{280} calibration of one rAAV for any serotype/payload combination by multiplying the ratio with a correction factor (CF$_{\%\text{full}}$). This factor can theoretically be determined by utilizing the extinction coefficients of both the capsid and the payload. However, due to the inherent complexity of rAAVs, these values are not easily accessible, and theoretical calculations based on the amino acid and nucleic acid sequences need at least be verified experimentally.

After having established a calibration curve for rAAV α (Figure 3, black curve) we determined CF$_{\%\text{full}}$ for rAAV β. The factor was obtained by analyzing a single SEC-MALS referenced sample of rAAV β containing filled capsids. The SEC-MALS derived %full was set in relation to the resulting %full applying the existing rAAV α calibration for the obtained A_{260}/A_{280} ratio according to Equation (7). Multiplying the existing calibration of rAAV α with the obtained CF$_{\%\text{full}}$ of 1.37 led to the %full calibration curve of rAAV β (Figure 3, black dotted line).
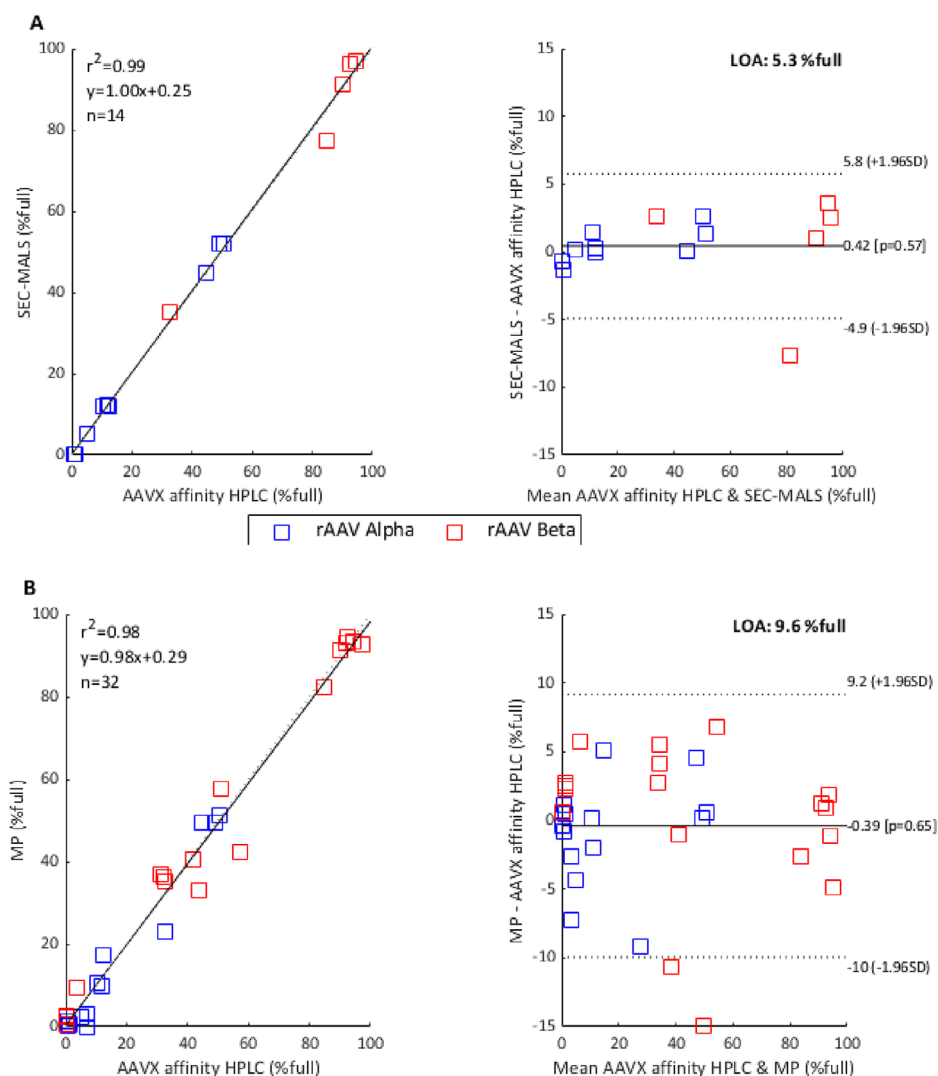
FIGURE 4 | Bland–Altman analysis comparing the results of %full determination by AAVX affinity HPLC against SEC-MALS (A) and MP (B) analysis. Each plot contains both the originally calibrated rAAV α (blue) and the recalibrated rAAV β (red). The bias (black line) of both Bland–Altman plots lies close to 0. Dotted lines display ±1.96 SD (standard deviation) confidence intervals for SEC-MALS and MP reference data. HPLC, high-performance liquid chromatography; MP, mass photometry; SEC-MALS, size exclusion chromatography coupled to multi-angle light scattering.

To confirm the validity of the herein proposed conversion for adapting the existing calibration of rAAV α to rAAV β, a set of various DSP samples with a broad range of titer and %full from both serotypes were analyzed by applying our affinity HPLC method. The obtained %full data were then compared against the corresponding SEC-MALS and, additionally, MP results using Bland–Altman analysis by calculating the difference of %full for two pairs of methods (here: AAVX affinity HPLC vs. SEC-MALS or MP) and plotting it against their means (Figure 4). The resulting bias (0.4% for comparison with SEC-MALS and −0.4% with MP) demonstrated a good agreement of our method with SEC-MALS and MP results for both the originally calibrated rAAV α and rAAV β whose calibration was derived by applying the previously mentioned conversion factor. Additionally, 95% of the differences are expected within a range of ±5% for comparison with SEC-MALS measurements (Figure 4A) and ±10% if compared to MP (Figure 4B). The higher deviation for MP measurements can be explained by the ability of MP to further differentiate between full and partially filled capsids.

By applying Equation (1) with %full derived from the A_{260}/A_{280} ratio, we were also able to determine the capsid titer in all samples of rAAV α and rAAV β that were collected during DSP. A comparison to SEC-MALS reference data (where available) again showed the alignment of both methods and the successful recalibration of rAAV β with the means of the existing calibration of rAAV α utilizing only two SEC-MALS referenced samples of rAAV β, one containing only empty capsids and the other one containing filled capsids (Figure 5).

3.2 | Analytical Assessment of rAAV Capsid Titer and %Full During Its Production

Titer and %full determination in fermentation broths is often hampered by low capsid titers and the high level of process-related impurities. Initial sample clarification applying centrifugation or filtration allows accessibility for analytical methods,
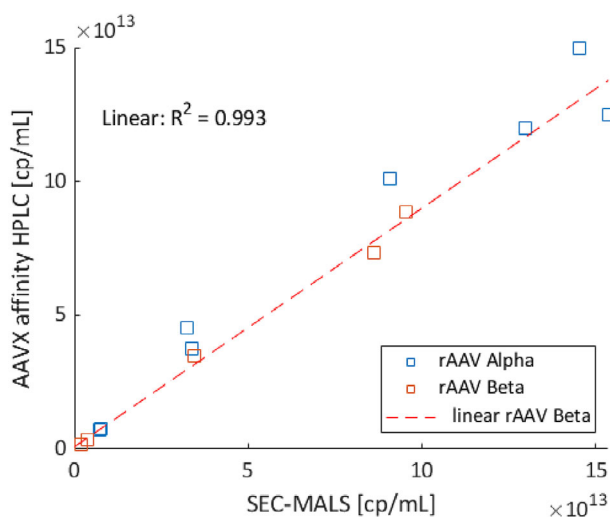
FIGURE 5 | Correlation of obtained results between AAVX affinity HPLC and SEC MALS. The determined capsid titers of various samples from the originally calibrated rAAV α and the recalibrated rAAV β showed good agreement ($R^2 = 0.993$) between both methods. rAAV, recombinant adeno-associated virus; SEC-MALS, size exclusion chromatography coupled to multiangle light scattering.

such as ELISA and q/ddPCR, which despite recent efforts to improve reproducibility still exhibit significant method variability [6].

By contrast, DSP of rAAVs typically involves a finely tuned succession of different unit operations [24, 25]. To concentrate the harvest volume and hence avoid high loading volumes for preparative chromatography, initial filtration of lysed cells by TFF is performed [26, 27]. Subsequent isolation of rAAV capsids is generally achieved through affinity chromatography allowing for selective binding of rAAV and consequently removal of impurities (e.g., host cell DNA/proteins and cell debris) [17, 28]. The captured capsids are then polished by AEX chromatography primarily to separate empty capsids from the desired fraction of full capsids, the latter being subjected to further processing and formulation [29–31].

The success of the different unit operations relies on the provision of precise analytical data in a timely manner, as titer information is exploited for the consecutive steps. Besides determining the capsid titer of elution pools for chromatographic operations to identify suitable process conditions, controlling the loading density is crucial to remove impurities both effectively and efficiently. In this context, column underloading can result in poor recovery due to undesired interactions and rebinding on the stationary phase, while overloading may lead to material loss and impaired removal of impurities.

Besides utilizing ELISA and q/ddPCR, titer and %full of purified samples can be obtained by SEC-MALS. In addition, MP analysis is used as this technique allows for discrimination between empty, full, and partially filled capsids. Nevertheless, process development and production timelines of rAAVs are affected by the TAT of these methods in analytical laboratories usually adding up to several days.

3.2.1 | Implementing AAVX Affinity HPLC as a Fast At-line Analytical Method During USP

In contrast to these established methods, adopting AAVX affinity HPLC, as introduced in a previous study, holds the prospect of offering a simple, fast, and widely applicable approach. To exploit its potential as an at-line tool for monitoring the capsid titer of an entire fermentation process, we collected and analyzed samples starting from 24 h after transfection until harvest at 96 h. For analysis, the drawn samples were either lysed or left untreated to determine the total rAAV titer and the amount of extracellular rAAVs, respectively.

Initial experiments were conducted by directly injecting the harvested cell culture fluid or its lysate onto the column. While these runs usually generated reproducible results, suggesting effective binding of the rAAVs, a gradual increase of system backpressure was observed potentially due to column clogging. As a consequence, we examined different approaches for sample clarification, specifically either through centrifugation or 0.22 μm filtration.

Overall, both clarification methods proved effective in removing cells, debris, and other impurities to an extent that column lifetime was no longer impaired. The total observed rAAV capsid titers attained after cell lysis were similar, with slightly higher titers (2%–8%) after sample filtration than after centrifugation. Comparing the extracellular titer of samples that were not lysed, the discrepancy between the two methods was more pronounced, with titers being higher between 13% and 66% in filtrated samples. This may be due to shear stress applied during filtration leading to cell disruption and consequently an increase of the obtained capsid titer. Considering these scenarios, centrifugation appeared to us as the preferred method for sample preparation, also due to its higher throughput and fewer manual sample handling steps. In addition to preceding sample clarification before analysis, we recommend the installation of an HPLC in-line filter. This helps to prevent column clogging and allows for quick cleaning by replacing the filter unit, thus helping to further extend column lifetime.

As shown in Figure 6, the total titer of rAAV increased throughout the fermentation process, reaching a plateau at approximately 72 h posttransfection. By contrast, the extracellular titer, approximately one order of magnitude lower than total titer, showed a steady increase after 72 h. The discrepancy observed between extracellular and total rAAV titer has already been described in literature and varies by 9%–88%, depending on the serotype and fermentation time [32–35]. Therefore, rAAV release by cell lysis is essential, as relying solely on the extracellular rAAV capsid titer in the cell culture broth may lead to an underestimation of the actual concentration and additionally, no direct correlation of the extracellular to the total capsid titer was found throughout the fermentation.

3.2.2 | Enabling PAT for DSP Unit Operations

3.2.2.1 | Process Yield Calculation. Analogous to the application of AAVX affinity HPLC during USP, we evaluated its
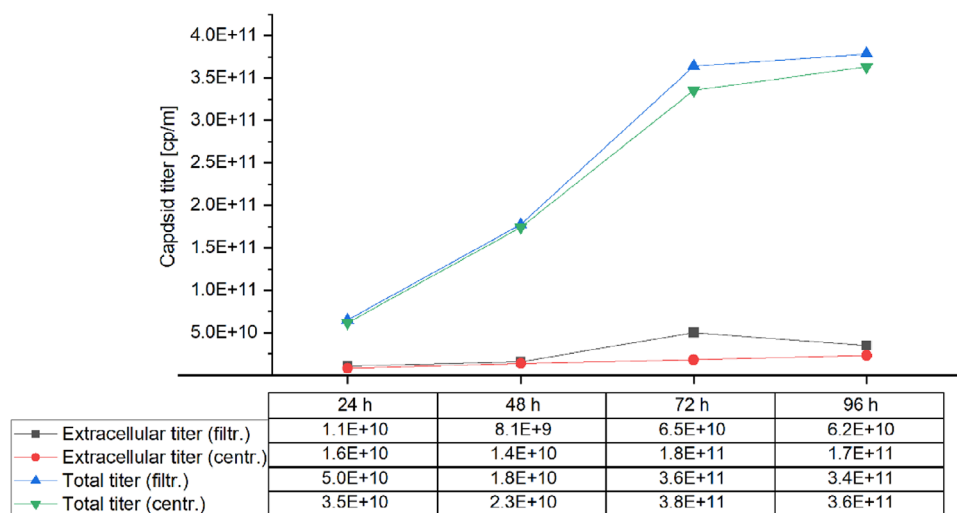
	24 h	48 h	72 h	96 h
Extracellular titer (filtr.)	1.1E+10	8.1E+9	6.5E+10	6.2E+10
Extracellular titer (centr.)	1.6E+10	1.4E+10	1.8E+11	1.7E+11
Total titer (filtr.)	5.0E+10	1.8E+10	3.6E+11	3.4E+11
Total titer (centr.)	3.5E+10	2.3E+10	3.8E+11	3.6E+11

FIGURE 6 | AAVX affinity HPLC analysis for upstream processing samples. Both extracellular and total capsid titer of rAAV β samples were determined on a daily basis during a 96 h fermentation. Before analysis, the samples were either filtrated or centrifuged for clarification. HPLC, high-performance liquid chromatography; rAAV, recombinant adeno-associated virus.

potential as a PAT tool for tracking the performance of DSP. First, the step and process yields for the entire downstream process, spanning various filtration and chromatography steps, were calculated for the two different serotypes rAAV α and rAAV β based on the obtained capsid titers and %full.

Resulting in a total yield of 17% capsids for rAAV α (Figure 7A) and 20% for rAAV β (Figure 7B), respectively, both processes exhibited a similar performance. Major losses of approximately 20% of rAAV capsids were observed during harvest concentration applying TFF. Affinity purification and subsequent AEX polishing caused losses of 15% per step unit. The %full only changed considerably during the separation of empty and full capsids employing AEX chromatography, whereas the slight fluctuations observed for harvest, TFF and AFF samples (as low as 3%) are attributed to the method variability. By contrast, the total capsid yield decreased for all steps, irrespective of the presence or absence of a DNA payload. For rAAV α, the AEX polishing was performed by applying step elution to separate empty and full capsids, resulting in 42% of full capsids in the pooled fraction (AEX FP). By contrast, polishing of rAAV β was performed by FT chromatorgraphy, for which the empty capsids were passed through the column during the load phase (AEX FT) followed by elution of the full capsids in two fractions, containing 57%full (AEX Elution 1) and 93%full (AEX Elution 2).

3.2.2.2 | AEX Process Development of rAAV α. Besides monitoring the overall yield during DSP, the fast TAT of our method facilitated streamlined process development of single-unit operations. This capability is exemplified by the optimization of the AEX chromatography step for rAAV α. By solely relying on the AAVX affinity HPLC results to adjust the chromatographic conditions, a significant improvement for the separation of empty and full capsids was achieved while performing three consecutive runs within 2 days. More specifically, the capsid yield of the targeted full pool increased from 24% to 37% while capsid separation improved as indicated by a higher %full (46% vs. 42%) of the respective fraction (Table 2).

3.2.2.3 | Single-Unit Operation Yield Calculation of rAAV β AEX. As further showcased, the AEX chromatography of rAAV β was optimized by taking advantage of the quickly available AAVX affinity HPLC results for process adjustments. In this example, the chromatography conditions were set in a manner that empty capsids passed through the column (FT fraction), whereas full capsids, preferentially retained on the column, were eluted in two fractions. In addition to the loading and elution fractions, the wash and cleaning-in-place (CIP 1 and CIP 2) steps were analyzed to get an overall picture of the capsid losses throughout the entire process (Figure 8). Notably, both runs were conducted within the same day.

The resulting mass balance for AEX run 1 indicated an FT of 51% of the loaded capsids, while a total of 34% of capsids was captured in the two pooled fractions. Nonetheless, a notable amount of payload containing capsids was not bound to the column in addition to an insufficient separation of full and empty capsids in fractions 1 (85%full) and 2 (90%full). For comparison, in the adjusted second run, the proportion of lost capsids during wash and CIP remained constant, while the amount of capsids in the FT decreased by 9% and we were able to capture 45% of the loaded capsids in the eluting fractions. Additionally, the FT showed no full capsids at all, while successful separation of empty and full capsids led to a fraction 2 displaying 94%full with an increase to 29% of the total yield. In both cases, we were able to track a total of >95% of capsids, which proves the high accuracy and sensitivity of the method for varying and also demanding sample compositions.

3.2.3 | PAT-Ability of At-Line AAVX Affinity HPLC Measurements

The identification and close monitoring of CQAs plays a fundamental role in ensuring consistent quality of (bio-)pharmaceuticals. Additionally, extensive knowledge about the manufacturing process and its impact on the CQAs allows for the definition of CPPs ultimately leading to well-controlled
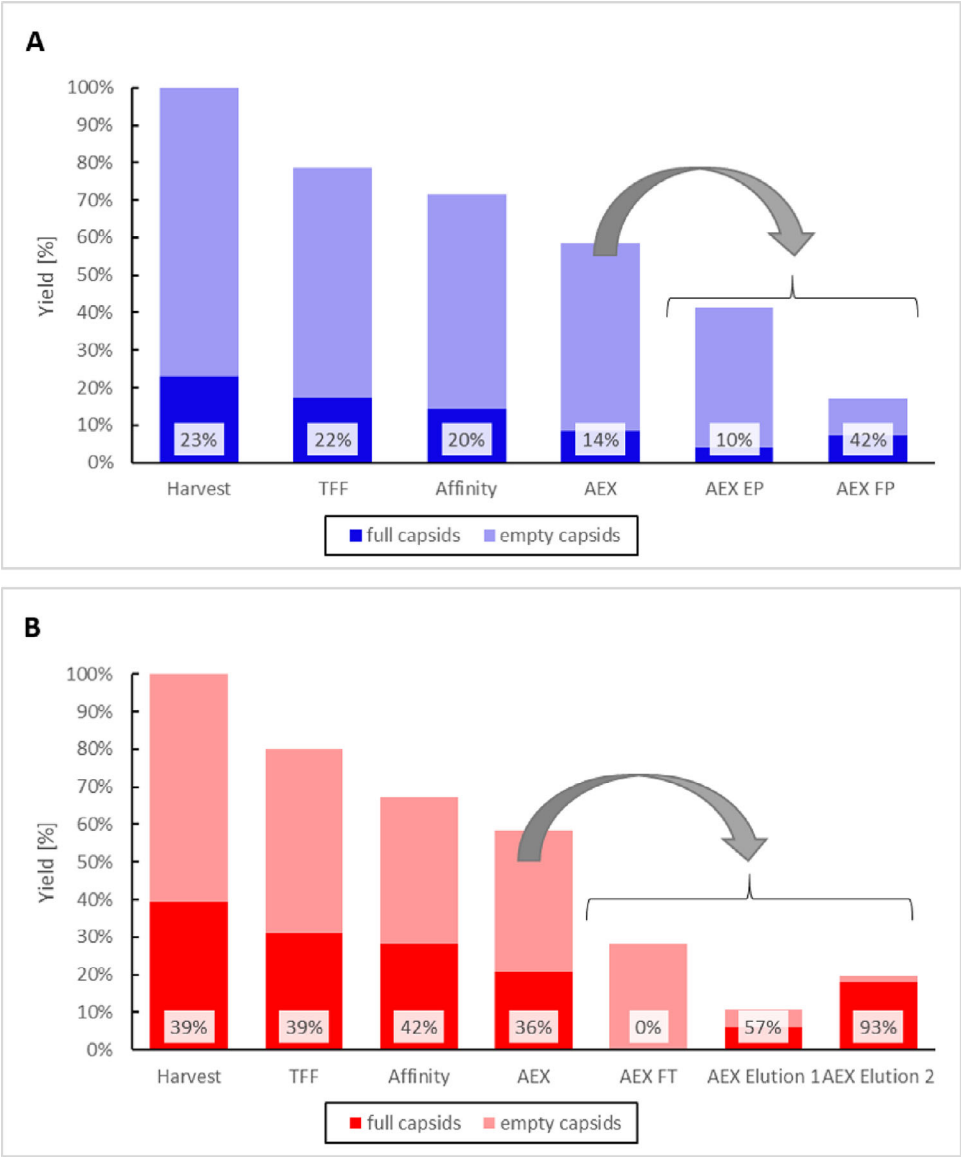
FIGURE 7 | Overall yield calculation based on at-line AAVX affinity HPLC analysis during DSP. Processing of rAAV α (A) and rAAV β (B) involved TFF, affinity purification, and AEX chromatography. For AEX chromatography, the obtained fractions are also displayed individually, including the empty (AEX EP) and full pool (AEX FP) for rAAV α and the flow-through fraction (AEX FT) as well as two elution fractions (AEX Elution 1 and AEX Elution 2) for rAAV β. The shown percentage values indicate %full in each fraction. AEX, anion exchange; DSP, downstream processing; HPLC, high-performance liquid chromatography; rAAV, recombinant adeno-associated virus; TFF, tangential flow filtration.

TABLE 2 | Capsid Yield and %full in AEX runs of rAAV α.

	Capsid yield			%full	
	Empty pool	**Full pool**	**Sum**	**Empty pool**	**Full pool**
AEX 1	58%	24%	82%	10%	42%
AEX 2	47%	29%	76%	2%	46%
AEX 3	37%	37%	75%	1%	46%

conditions for each unit operation. In rAAV-based gene therapies, the capsid titer and %full are arguably among the most important CQAs, as they directly impact the efficacy of the product.

PAT is an approach that integrates analytical methods into the process to monitor relevant process parameters or product attributes. Applying such methods, it fosters a deeper process understanding and offers the possibility of enhanced process
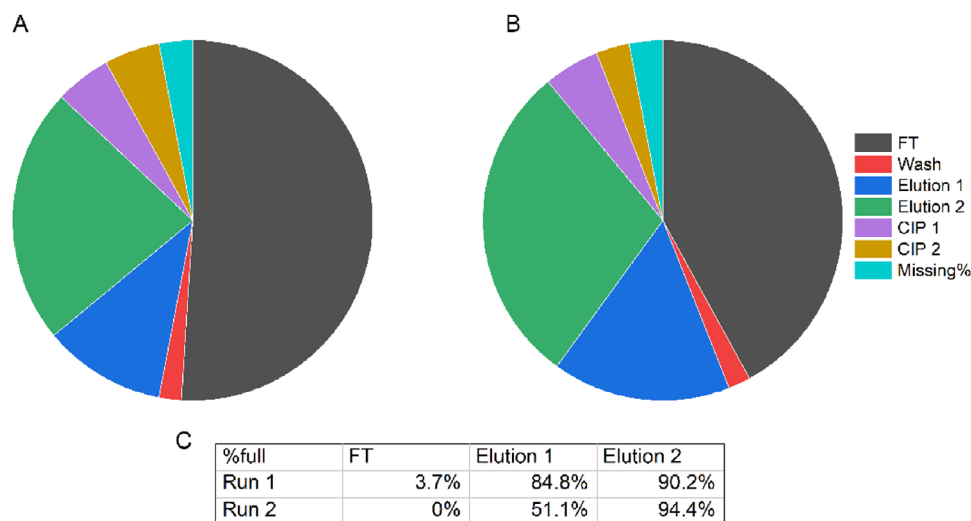
FIGURE 8 | Mass balance for two AEX chromatography runs of rAAV β. The capsid titer of run 1 (A) and run 2 (B) was determined in the FT, wash, Elution 1, Elution 2, CIP 1, and CIP 2 fractions applying AAVX Affinity HPLC. %full determination (C) was limited to the FT, Elution 1, and Elution 2 fractions. The results from the first run were directly utilized to perform run 2 under optimized conditions on the same day. Missing% in (A) and (B) refers to the deviation from the loaded amount. CIP, cleaning in place; FT, flow-through; HPLC, high-performance liquid chromatography.

control. While the implementation of PAT is generally advocated by health authorities and the increased demand for such tools was clearly highlighted in recent publications, there is still a lack of suitable methods that can perform this task for rAAV-based gene therapy products [6, 36, 37, 38]. This is mainly due to a lack of sensitivity, long TATs, or signal interferences by sample impurities for existing analytical techniques.

To address this gap and potentially enable PAT in development and production of rAAV-based gene therapies, we assessed the suitability of our previously published AAVX affinity HPLC method as an at-line tool for monitoring capsid titer and %full during both fermentation and DSP of different rAAV serotypes. Taking advantage of the isolation and subsequent elution of the entire rAAV fraction in a single peak, this approach proved highly efficient in removing process-related impurities as well as affording analysis under steady conditions irrespective of the sample composition. In addition, through the sharp elution profile, the rAAVs are concentrated, which extends potential applications of the method.

During USP, samples generally display low titers and high levels of impurities and additionally require preparation steps prior to analysis, such as cell lysis and subsequent clarification via filtration or centrifugation. As demonstrated, our method allowed for determining the capsid titer and %full during fermentation within a short timeframe of less than 1 h, thereby supporting process monitoring and prediction of the optimal harvest time. Given the potential for high-throughput analysis, it is conceivable that our method is additionally well suited for screening cell culture conditions to achieve high capsid yields.

To obtain high temporal resolution of downstream processes, the sampling frequency needs to be considerably higher compared to fermentation, depending on the employed unit operation. In addition, the attained information from the previous processing step is often used to calculate or adjust the conditions applied for the following unit operation. These characteristics presuppose

fast provision of analytical results in order to facilitate seamless and efficient workflows. However, the established analytical methods to determine capsid titer and %full of AAVs, with typical TAT in analytical laboratories of several days up to weeks, are inapt to perform this task. By contrast, operating our AAVX affinity method in close proximity to the downstream process, the fast run time of less than 5 min could be exploited to inform downstream engineers about the results immediately after each processing step.

Additionally, analysis of FT fractions during loading or washing steps can support the optimization of process conditions to reduce product loss. Again, common analytical technologies such as SEC-MALS or MP are not suitable for these kind of samples due to low titers, high levels of impurities, or harsh sample conditions resulting in impaired method reliability. Combining the analytical results for different unit operations allows for the determination of the step yield and the overall process yield, which in turn facilitates comprehensive process understanding.

Overall, the insights provided in this work highlight the method's ability to reliably analyze diverse samples throughout the entire production process. Comparing duplicate measurements of samples in the DSP case study showed high repeatability with precision of 95% and 99% for capsid concentrations below and above 1.5E11 cp/mL, respectively. The hereby obtained findings were later affirmed by SEC-MALS and MP reference measurements.

4 | Conclusion

Starting with fermentation at 24 h posttransfection followed by harvest over filtration, concentration, affinity-based purification, and concluding with an AEX polishing step, our AAVX affinity HPLC method was applied for monitoring the rAAV capsid titer and %full. The clear advantage of our methods was demonstrated in its broad applicability to analyze samples derived from different process stages at-line ranging from samples containing various

impurities and low titers (e.g., USP samples) or unfavorable sample conditions (e.g., high salt strip during DSP) with high precision and with a TAT of less than 5 min per analyzed sample.

Consequently, all results were available within minutes after each process unit operation with high sensitivity, specificity, and reproducibility. Therefore, the AAVX affinity HPLC method not only conduces to better process understanding but also saves time, as results can be immediately used to plan and execute subsequent processing steps. With the potential for online application and even shorter TAT of 2 min per analysis as demonstrated recently, this method is the first of its kind paving the way for PAT in rAAV-based gene therapies [39].

Conflicts of Interest

J.H., T.B., L.B., M.L., M.H., and T.G. are current employees of Roche Diagnostics GmbH and some of whom declare stock ownership in the Roche Holding AG.

Ethics Statement

Patient consent statement, permission to reproduce material from other sources, and clinical trial registration are not applicable.

Data Availability Statement

Roche Diagnostics GmbH is unable to provide materials, additional datasets, or protocols.

References

1. M. F. Naso, B. Tomkowicz, W. L. Perry, and W. R. Strohl, "Adeno-Associated Virus (AAV) as a Vector for Gene Therapy," *Biodrugs* 31, no. 4 (2017): 317–334, https://doi.org/10.1007/s40259-017-0234-5.

2. D. Wang, P. W. L. Tai, and G. Gao, "Adeno-Associated Virus Vector as a Platform for Gene Therapy Delivery," *Nature Reviews Drug Discovery* 18, no. 5 (2019): 358–378, https://doi.org/10.1038/s41573-019-0012-9.

3. T. Burdett and S. Nuseibeh, "Changing Trends in the Development of AAV-Based Gene Therapies: A Meta-Analysis of Past and Present Therapies," *Gene Therapy* 30, no. 3–4 (2023): 323–335, https://doi.org/10.1038/s41434-022-00363-0.

4. T. Tanaka, H. Hanaoka, and S. Sakurai, "Optimization of the Quality by Design Approach for Gene Therapy Products: A Case Study for Adeno-Associated Viral Vectors," *European Journal of Pharmaceutics and Biopharmaceutics* 155 (2020): 88–102, https://doi.org/10.1016/j.ejpb.2020.08.002.

5. A. S. Rathore, R. Bhambure, and V. Ghare, "Process Analytical Technology (PAT) for Biopharmaceutical Products," *Analytical and Bioanalytical Chemistry* 398, no. 1 (2010): 137–154, https://doi.org/10.1007/s00216-010-3781-x.

6. A. L. Gimpel, G. Katsikis, and S. Sha, et al., "Analytical Methods for Process and Product Characterization of Recombinant Adeno-Associated Virus-Based Gene Therapies," *Molecular Therapy—Methods & Clinical Development* 20 (2021): 740–754, https://doi.org/10.1016/j.omtm.2021.02.010.

7. J. F. Wright, "Quality Control Testing, Characterization and Critical Quality Attributes of Adeno-Associated Virus Vectors Used for Human Gene Therapy," *Biotechnology Journal* 16, no. 1 (2021): 2000022, https://doi.org/10.1002/biot.202000022.

8. W. Chew and P. Sharratt, "Trends in Process Analytical Technology," *Analytical Methods* 2, no. 10 (2010): 1412–1438, https://doi.org/10.1039/c0ay00257g.

9. D. A. M. Pais, C. Brown, A. Neuman, et al., "Dielectric Spectroscopy to Improve the Production of rAAV Used in Gene Therapy," *Processes* 8, no. 11 (2020): 1456, https://doi.org/10.3390/pr8111456.

10. D. A. M. Pais, R. M. C. Portela, M. J. T. Carrondo, I. A. Isidro, and P. M. Alves, "Enabling PAT in Insect Cell Bioprocesses: In Situ Monitoring of Recombinant Adeno-Associated Virus Production by Fluorescence Spectroscopy," *Biotechnology and Bioengineering* 116, no. 11 (2019): 2803–2814, https://doi.org/10.1002/bit.27117.

11. C. F. Iglesias, M. Ristovski, M. Bolic, and M. Cuperlovic-Culf, "rAAV Manufacturing: The Challenges of Soft Sensing During Upstream Processing," *Bioengineering* 10, no. 2 (2023): 229, https://doi.org/10.3390/bioengineering10020229.

12. T. Williams, K. Kalinka, R. Sanches, et al., "Machine Learning and Metabolic Modelling Assisted Implementation of a Novel Process Analytical Technology in Cell and Gene Therapy Manufacturing," *Scientific Reports* 13, no. 1 (2023): 834, https://doi.org/10.1038/s41598-023-27998-2.

13. J. Heckel, A. Martinez, and C. Elger, et al., "Fast HPLC-Based Affinity Method to Determine Capsid Titer and Full/Empty Ratio of Adeno-Associated Viral Vectors," *Molecular Therapy—Methods & Clinical Development* 31 (2023): 101148, https://doi.org/10.1016/j.omtm.2023.101148.

14. E. H. T. M. Ebberink, A. Ruisinger, M. Nuebel, M. Thomann, and A. J. R. Heck, "Assessing Production Variability in Empty and Filled Adeno-Associated Viruses by Single Molecule Mass Analyses," *Molecular Therapy—Methods & Clinical Development* 27 (2022): 491–501, https://doi.org/10.1016/j.omtm.2022.11.003.

15. D. Wu, P. Hwang, T. Li, and G. Piszczek, "Rapid Characterization of Adeno-Associated Virus (AAV) Gene Therapy Vectors by Mass Photometry," *Gene Therapy* 29, no. 12 (2022): 691–697, https://doi.org/10.1038/s41434-021-00311-4.

16. G. D. Florencio, G. Precigout, C. Beley, P. O. Buclez, L. Garcia, and R. Benchaouir, "Simple Downstream Process Based on Detergent Treatment Improves Yield and in Vivo Transduction Efficacy of Adeno-Associated Virus Vectors," *Molecular Therapy—Methods & Clinical Development* 2 (2015): 15024, https://doi.org/10.1038/mtm.2015.24.

17. M. Florea, F. Nicolaou, and S. Pacouret, et al., "High-Efficiency Purification of Divergent AAV Serotypes Using AAVX Affinity Chromatography," *Molecular Therapy—Methods & Clinical Development* 28 (2023): 146–159, https://doi.org/10.1016/j.omtm.2022.12.009.

18. A. B. T. Ghisaidoobe and S. J. Chung, "Intrinsic Tryptophan Fluorescence in the Detection and Analysis of Proteins: A Focus on Förster Resonance Energy Transfer Techniques," *International Journal of Molecular Sciences* 15, no. 12 (2014): 22518–22538, https://doi.org/10.3390/ijms151222518.

19. Y. Xie and M. Butler, "Multi-Attribute Analysis of Adeno-Associated Virus by Size Exclusion Chromatography With Fluorescence and Triple-Wavelength UV Detection," *Analytical Biochemistry* 680 (2023): 115311, https://doi.org/10.1016/j.ab.2023.115311.

20. N. L. McIntosh, G. Y. Berguig, O. A. Karim, et al., "Comprehensive Characterization and Quantification of Adeno Associated Vectors by Size Exclusion Chromatography and Multi Angle Light Scattering," *Scientific Reports* 11, no. 1 (2021): 3012, https://doi.org/10.1038/s41598-021-82599-1.

21. B. Troxell, I. W. Tsai, K. Shah, et al., "Application of Size Exclusion Chromatography With Multiangle Light Scattering in the Analytical Development of a Preclinical Stage Gene Therapy Program," *Human Gene Therapy* 34, no. 7–8 (2023): 325–338, https://doi.org/10.1089/hum.2022.218.

22. G. A. Rodrigues, E. Shalaev, T. K. Karami, J. Cunningham, N. K. H. Slater, and H. M. Rivers, "Pharmaceutical Development of AAV-Based Gene Therapy Products for the Eye," *Pharmaceutical Research* 36, no. 2 (2019): 29, https://doi.org/10.1007/s11095-018-2554-7.

23. J. M. Sommer, P. H. Smith, S. Parthasarathy, et al., "Quantification of Adeno-Associated Virus Particles and Empty Capsids by Optical Density Measurement," *Molecular Therapy* 7, no. 1 (2003): 122–128, https://doi.org/10.1016/s1525-0016(02)00019-9.

24. B. Adams, H. Bak, and A. D. Tustian, "Moving From the Bench Towards a Large Scale, Industrial Platform Process for Adeno-Associated Viral Vector Purification," *Biotechnology and Bioengineering* 117, no. 10 (2020): 3199–3211, https://doi.org/10.1002/bit.27472.

25. J. E. Andari and D. Grimm, "Production, Processing, and Characterization of Synthetic AAV Gene Therapy Vectors," *Biotechnology Journal* 16, no. 1 (2021): e2000025, https://doi.org/10.1002/biot.202000025.

26. D. L. Grzenia, J. O. Carlson, and S. R. Wickramasinghe, "Tangential Flow Filtration for Virus Purification," *Journal of Membrane Science* 321, no. 2 (2008): 373–380, https://doi.org/10.1016/j.memsci.2008.05.020.

27. R. Miyaoka, Y. Tsunekawa, Y. Kurosawa, et al., "Development of a Novel Purification Method for AAV Vectors Using Tangential Flow Filtration," *Biotechnology and Bioengineering* 120, no.11 (2023): 3311–3321, https://doi.org/10.1002/bit.28524.

28. M. Toueille, L. Dejoint, E. Attebi, et al., "Development of Purification Steps for Several AAV Serotypes Using POROS™ CaptureSelect™ AAVX Affinity Chromatography," *Cell and Gene Therapy Insights* 4, no. 7 (2018): 637–645, https://doi.org/10.18609/cgti.2018.061.

29. R. Dickerson, C. Argento, J. Pieracci, and M. Bakhshayeshi, "Separating Empty and Full Recombinant Adeno-Associated Virus Particles Using Isocratic Anion Exchange Chromatography," *Biotechnology Journal* 16, no. 1 (2021): e2000015, https://doi.org/10.1002/biot.202000015.

30. W. Di, K. Koczera, P. Zhang, D. P. Chen, J. C. Warren, and C. Huang, "Improved Adeno-Associated Virus Empty and Full Capsid Separation Using Weak Partitioning Multi-Column AEX Chromatography," *Biotechnology Journal* 19, no. 1 (2024): e2300245, https://doi.org/10.1002/biot.202300245.

31. P. R. H. Joshi, A. Bernier, P. D. Moço, J. Schrag, P. S. Chahal, and A. Kamen, "Development of a Scalable and Robust AEX Method for Enriched rAAV Preparations in Genome-Containing VCs of Serotypes 5, 6, 8, and 9," *Molecular Therapy—Methods & Clinical Development* 21 (2021): 341–356, https://doi.org/10.1016/j.omtm.2021.03.016.

32. M. J. Benskey, I. M. Sandoval, and F. P. Manfredsson, "Continuous Collection of Adeno-Associated Virus from Producer Cell Medium Significantly Increases Total Viral Yield," *Human Gene Therapy Methods* 27, no. 1 (2016): 32–45, https://doi.org/10.1089/hgtb.2015.117.

33. T. Okada, M. Nonaka-Sarukawa, R. Uchibori, et al., "Scalable Purification of Adeno-Associated Virus Serotype 1 (AAV1) and AAV8 Vectors, Using Dual Ion-Exchange Adsorptive Membranes," *Human Gene Therapy* 20, no. 9 (2009): 1013–1021, https://doi.org/10.1089/hum.2009.006.

34. B. A. Piras, J. E. Drury, C. L. Morton, et al., "Distribution of AAV8 Particles in Cell Lysates and Culture Media Changes With Time and Is Dependent on the Recombinant Vector," *Molecular Therapy—Methods & Clinical Development* 3 (2016): 16015, https://doi.org/10.1038/mtm.2016.15.

35. L. H. Vandenberghe, R. Xiao, M. Lock, J. Lin, M. Korn, and J. M. Wilson, "Efficient Serotype-Dependent Release of Functional Vector into the Culture Medium During Adeno-Associated Virus Manufacturing," *Human Gene Therapy* 21, no. 10 (2010): 1251–1257, https://doi.org/10.1089/hum.2010.107.

36. P. Cashen and K. McLaughlin, "Overview of Current Downstream Processing for Modern Viral Vectors," in *Bioprocess and Analytics Development for Virus-Based Advanced Therapeutics and Medicinal Products (ATMPs)* (Springer, 2023), 91–123, https://doi.org/10.1007/978-3-031-28489-2_5.

37. Z. Jiang and P. A. Dalby, "Challenges in Scaling up AAV-Based Gene Therapy Manufacturing," *Trends in Biotechnology* 41, no. 10 (2023): 1268–1281, https://doi.org/10.1016/j.tibtech.2023.04.002.

38. J. Ou, Y. Tang, J. Xu, J. Tucci, M. C. Borys, and A. Khetan, "Recent Advances in Upstream Process Development for Production of Recombinant Adeno-Associated Virus," *Biotechnology and Bioengineering* 121, no. 1 (2024): 53–70, https://doi.org/10.1002/bit.28545.

39. T. Graf, L. Naumann, L. Bonnington, et al., "Expediting Online Liquid Chromatography for Real-Time Monitoring of Product Attributes to Advance Process Analytical Technology in Downstream Processing of Biopharmaceuticals," *Journal of Chromatography A* 1729 (2024): 465013, https://doi.org/10.1016/j.chroma.2024.465013.

Supporting Information

Additional supporting information can be found online in the Supporting Information section.